Polysaccharide Processing and Presentation by the MHCII Pathway

Brian A. Cobb,[1,2] Qun Wang,[1,2]
Arthur O. Tzianabos,[1] Dennis L. Kasper[1,2,*]
[1]Channing Laboratory
Department of Medicine
Brigham & Women's Hospital
Boston, Massachusetts 02115
[2]Department of Microbiology and
    Molecular Genetics
Harvard Medical School
Boston, Massachusetts 02115

Summary

The adaptive immune system functions through the combined action of antigen-presenting cells (APCs) and T cells. Specifically, class I major histocompatibility complex antigen presentation to CD8^{+} T cells is limited to proteosome-generated peptides from intracellular pathogens while the class II (MHCII) endocytic pathway presents only proteolytic peptides from extracellular pathogens to CD4^{+} T cells. Carbohydrates have been thought to stimulate immune responses independently of T cells; however, zwitterionic polysaccharides (ZPSs) from the capsules of some bacteria can activate CD4^{+} T cells. Here we show that ZPSs are processed to low molecular weight carbohydrates by a nitric oxide-mediated mechanism and presented to T cells through the MHCII endocytic pathway. Furthermore, these carbohydrates bind to MHCII inside APCs for presentation to T cells. Our observations begin to elucidate the mechanisms by which some carbohydrates induce important immunologic responses through T cell activation, suggesting a fundamental shift in the MHCII presentation paradigm.

Introduction

Recognition of foreign extracellular proteins by the adaptive immune system begins with their entry into professional APCs (i.e., dendritic cells, macrophages, and B cells) and depends upon antigen processing through the MHCII endocytic pathway and subsequent presentation to CD4^{+} T cells (Watts and Powis, 1999). Most pathogens initially undergo endocytosis by the APCs and are subsequently killed by oxidant molecules (e.g., superoxide and nitric oxide) produced during the oxidative burst (Forman and Torres, 2001). Endosomes carrying released proteins then move through the vesicular traffic, fusing with acidic lysosomes carrying host proteases (Watts, 1997). These endo/lysosomes subsequently fuse with exocytic vesicles, forming the MHCII compartment (MIIC). Exocytic vesicles originate in the trans-Golgi network and contain proteins such as the MHCII protein HLA-DR, accessory proteins like the MHCII bound invariant chain (Ii), and HLA-DM (Watts, 1997). Within the MIIC, the lysosomal proteases process the

pathogen-derived proteins to peptides and cleave Ii away from MHCII, leaving an Ii-derived self-peptide (CLIP) in the antigen binding groove of MHCII (Shi et al., 1992, 1999). The acidic pH also activates HLA-DM to catalyze the exchange of CLIP for antigenic peptides (Busch et al., 1998). Finally, the MHCII-peptide complex is shuttled to the cell surface where it is recognized by $\alpha\beta$ T cell receptors ($\alpha\beta$TCRs) on CD4^{+} T cells, generating a specific immune response.

Adaptive MHCII-mediated CD4^{+} T cell activation has been considered to be strictly limited to protein antigens (Watts and Powis, 1999). When presented to T cells by MHCII, peptide antigens generally elicit a T cell-dependent immune response typified by the production of Th1 or Th2 cytokines as well as IgG and the induction of immunologic memory. In contrast, the immunologic response to polysaccharide antigens is considered T cell independent and characterized by a primary humoral immune response of IgM production, rare IgG class switching, and no immunologic memory (Abbas et al., 2000). Vaccine research with carbohydrate-protein conjugates has demonstrated that attachment of some polysaccharides or oligosaccharides to immunogenic carrier proteins like tetanus toxoid can generate an antigen capable of inducing significant IgG production (Kasper et al., 1996), T cell activation, and immune memory specifically directed toward the carbohydrate (Baker et al., 1999). However, no immunologic model exists that describes T cell-dependent immune responses generated by carbohydrates in the absence of a carrier protein.

In a rodent model of intraabdominal abscess formation, it was shown that the activation of CD4^{+} $\alpha\beta$ T cells by capsular polysaccharides is required for the modulation of abscess formation (Tzianabos et al., 2001). Experiments designed to study abscess formation resulting from colonic perforation demonstrated that mice lacking CD4^{+} T cells failed to develop abscesses in response to purified polysaccharides with an adjuvant of sterilized cecal contents (SCC) to mimic colonic leakage, yet transfer of naïve CD4^{+} T cells into these animals restored the animal's ability to develop abscesses in response to polysaccharides and SCC (Chung et al., 2003). Polysaccharide-mediated T cell activation can also be measured in vitro by monitoring T cell proliferation (Tzianabos et al., 2000) or production of cytokines such as IL-2, IL-10, and interferon γ (Tzianabos et al., 1999). Furthermore, CD4^{+} T cells activated by polysaccharides in vitro induce abscesses when given intraperitoneally with adjuvant; however, intravenous transfer of these same activated T cells without adjuvant conferred protection against abscesses induced by viable bacteria (Tzianabos and Kasper, 2002). These studies established that some polysaccharides can activate CD4^{+} T cells in vivo and in vitro.

Chemical characterization of several polysaccharides able to activate T cells has shown that the common characteristic is the presence of a zwitterionic charge motif within the repeating unit. These zwitterionic polysaccharides (ZPSs) are inactivated by chemical modifi-

*Correspondence: dennis_kasper@hms.harvard.edu

cations that eliminate the alternating charge character of the carbohydrate. Conversely, neutral or negatively charged polysaccharides do not show an ability to activate T cells or facilitate abscess formation, yet if chemically altered to be zwitterionic, this immunologic activity is created (Tzianabos et al., 1993). NMR structural studies of ZPSs such as polysaccharide A (PS-A) from *B. fragilis* and the capsular polysaccharide from type 1 *Streptococcus pneumoniae* (Sp1) reveal the formation of extended right-handed helices in solution (Wang et al., 2000; Choi et al., 2002). These helices have repeated 15 Å negatively charged grooves whose lateral boundaries are occupied by the charges, with the positive charges located on the outer surfaces. The molecular weight (MW) of ZPSs has been shown to impact antigenicity in that ZPSs of ≤5 kDa appear to poorly activate T cells, while those of ≥15 kDa activate to equal extents (Kalka-Moll et al., 2000). These studies collectively suggest that the epitope in abscess-inducing ZPSs is both structural and electrostatic in nature.

In vitro T cell activation assays with fixed APCs fail to activate T cells; thus, like a conventional protein antigen, ZPS molecules require entry into the APC (Brubaker et al., 1999). It was further demonstrated that T cell activation by ZPS molecules requires endo/lysosomal acidification in addition to the MHCII protein HLA-DR—but not HLA-DP, HLA-DQ, or any of the MHC class I molecules (Kalka-Moll et al., 2002). Given that acidic intravesicular pH is required for protease activity and invariant chain (Ii) cleavage (Shi et al., 1992, 1999), HLA-DM activity (Busch et al., 1998), and HLA-DR antigen binding activity (Rotzschke et al., 2002), these data raise the possibility that ZPS-mediated T cell activation occurs via the conventional MHCII endocytic pathway.

In this report, we describe the pathway utilized by ZPS antigens to activate T cells. Our results indicate that PS-A is endocytosed by APCs and localizes to the conventional MIIC. Biochemical, coimmunoprecipitation (co-IP), and animal studies demonstrate ZPS processing through oxidation by nitric oxide (NO). We further show that PS-A requires entry, MIIC acidification, processing, and MHCII expression for presentation by B cells and T cell engagement via interactions with αβTCRs. Finally, we present data that demonstrate that PS-A binds to MHCII in a pH-, HLA-DM-, and processing-sensitive manner. These data form the basis for a substantial broadening of the paradigm of MHCII processing and presentation to include non-protein antigens and oxidative antigen processing.

Results

Polysaccharide Antigens Are Taken into the MHC Class II Endocytic Pathway

To understand the role of the MHCII endocytic pathway in polysaccharide-mediated T cell responses, we studied ZPS trafficking in APCs. Using confocal microscopy with human Raji B cells, we found significant amounts of PS-A both inside and on the surface of APCs (Figure 1A). Time course studies indicated that entry and surface localization of PS-A was visible in 30 min and peaked at 6 hr (not shown), while Z axis optical slices confirmed that the PS-A signal is both inside the cell and

coating the surface (not shown). In addition, significant surface and intracellular regions of colocalization indicated that ZPS and MHCII proteins colocalize intracellularly as well as on the plasma membrane (Figure 1A, arrowhead and arrows, respectively). In order to eliminate the possibility that these observations were limited to cultured Raji cells, human peripheral blood mononuclear cells (PBMCs; Figure 1B) and mouse splenocytes (not shown) were also used to demonstrate colocalization of MHCII and PS-A. Control studies with ovalbumin showed both entry and surface colocalization with MHCII, yet neutral and negatively charged polysaccharide controls showed entry but failed to colocalize on the surface with MHCII (not shown).

Endosomes are known to fuse with lysosomes as well as exocytic vesicles from the trans-Golgi network carrying the MHCII machinery in the established MHCII pathway (Watts, 1997); however, the involvement of these vesicles in the trafficking of ZPS antigens was not known. Using mAbs to the lysosomal marker LAMP-1 (D'Souza and August, 1986) and the exocytic vesicle marker HLA-DM (Sanderson et al., 1994), we found that PS-A colocalized with both LAMP-1 (Figure 1C) and HLA-DM (Figure 1D) inside the cells.

Endocytosis and phagocytosis are processes that require cytoskeletal rearrangements and polymerization. In order to distinguish passive entry across or through membrane proteins from classical endocytosis, drugs known to inhibit cytoskeleton polymerization were used. Raji cells were first treated with either cytochalasin D to block actin polymerization (Figure 1E, left) or colchicine to block microtubule polymerization (Figure 1E, middle) and then incubated with PS-A and stained with mAbs to HLA-DR. As previously seen for conventional protein antigens (Bacci et al., 1996; Svensson et al., 1997), both of these inhibitors significantly reduced the endocytosis of PS-A (Figure 1E, right).

Another key step in the established MHCII pathway is the acidification of the MIIC vesicle, which is required to free the peptide binding site on MHCII proteins (Riberdy et al., 1992; Sloan et al., 1995). To assess the impact of acidification on ZPS progress in the endocytic pathway, Raji cells were treated with either bafilomycin A1 (BFA; Figure 1F, left), an inhibitor of the ATPase proton pump, or chloroquine (Figure 1F, middle), which buffers the vesicles and prevents acidification indirectly. Similar to conventional antigens, we found that these treatments did not reduce the amount of ZPS endocytosed or the colocalization of ZPS with MHCII proteins within the MIIC compartment (Figure 1F, right).

Although MHCII and PS-A colocalization was observed, it was not clear whether this was due to fusion of exocytic vesicles with endo/lysosomes or to entry of the PS-A-loaded vesicles into the ER through an unknown mechanism. These possibilities were examined in cells treated with brefeldin A, which blocks trafficking between the Golgi apparatus and the ER, with the net effect of trapping proteins inside the ER following their synthesis (Adorini et al., 1990). We found that uptake of PS-A was not significantly affected, yet MHCII and PS-A colocalization was reduced (Figure 1G, left) in a dose-dependent manner (Figure 1G, right).
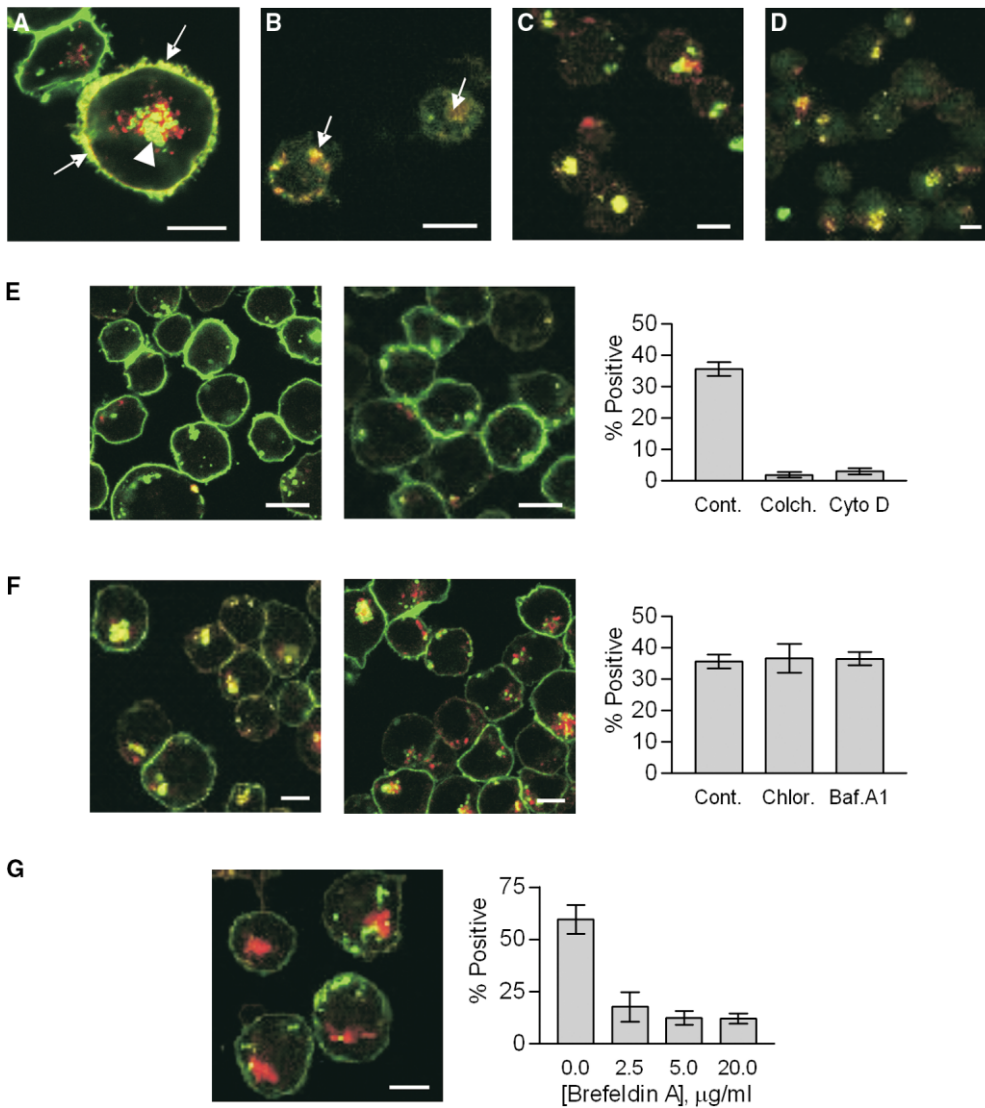
Figure 1. Trafficking of ZPS Antigens

Fluorescent antigens (red) were incubated with APCs and then with fluorescent mAbs against host markers (green). Yellow signal indicates colocalization. White bars indicate 10 μm.

(A) PS-A in Raji cells stained for HLA-DR, showing internal (arrow heads) and surface (arrows) colocalization.

(B) Primary human MNCs with PS-A and HLA-DR colocalized (arrows).

(C) Raji cells with PS-A and LAMP-1 colocalized (yellow).

(D) Raji cells with PS-A and HLA-DM with colocalization (yellow).

(E) Raji cells with the actin inhibitor cytochalasin D (left) or the microtubule inhibitor colchicine (middle) reduced PS-A uptake and HLA-DR colocalization (p < 0.0001; right).

(F) Raji cells with either bafilomycin A1 (left) or chloroquine (middle) showing no significant change (p = 0.7852) in PS-A/HLA-DR colocalization (right).

(G) Raji cells with brefeldin A (20 μg/ml; left). Intracellular and surface colocalization is impaired (p < 0.0001; right), yet uptake of antigen is not altered.

Polysaccharide Antigens Are Partially Depolymerized inside Endocytic Compartments

Protein antigens are digested by acid-activated proteases in the MIIC vesicle for peptide generation and loading onto MHCII for presentation. In order to determine if ZPS molecules are also processed, B cells (Raji and M12) were incubated with [³H]-PSA overnight, then the microsomal fractions of the cells were analyzed to measure the MW of recovered PS-A. We found that both cell lines depolymerized PS-A from >100 kDa to a MW of about 15 kDa (Figure 2A, arrow). This observation was confirmed in primary mouse splenocytes, THP-1 monocytes, and B1 B cells (not shown). The low MW radioactive polysaccharide recovered was immunoprecipitated with specific serum, which demonstrated that both the high and low MW PS-A were recognized to the same degree (not shown).

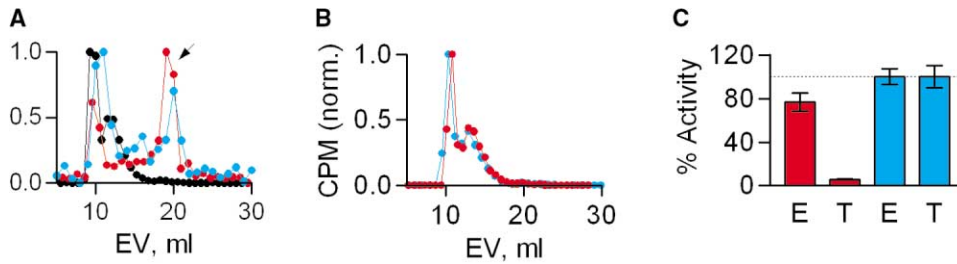Elucidation of the mechanism for PS-A processing

Figure 2. Polysaccharide Processing

EV is the elution volume in ml.

(A) [³H]-PSA isolated from Raji (red) or M12 (blue) B cell endosomes analyzed by Superose 12 chromatography. Control PS-A (black) eluted at the void volume of the column (MW >100 kDa). PS-A isolated from either B cell line showed both high and low (arrow; ~15 kDa) MW fragments and retained recognition by PS-A mAbs (not shown).

(B) [³H]-PSA incubated with Raji endo/lysosomal lysates (blue) and control [³H]-PSA (red) analyzed by Superose 12, showing no enzymatic cleavage.

(C) The same endo/lysosomal lysates (E) show acid-stable protease activity unlike trypsin (T). Red and blue bars indicate assays performed at pH 5.0 and pH 7.3, respectively. Data were normalized to the pH 7.3 activity.

was first explored through the use of microsomal lysates. The possibility of glycosidase activity was measured with lysate-treated [³H]-PSA under neutral and acidic conditions. Using Superose 12 chromatography, we found no detectable processing activity in any of the assayed lysates (Figure 2B), yet these same lysates consistently showed acid-stable protease activity (Figure 2C).

Next, the effects of the environmental conditions found along the endocytic pathway on PS-A were studied. As summarized in Figure 3A, we found that neither low pH (4.5 to 5.0) nor reducing conditions (2-mercaptoethanol) had a measurable effect on PS-A. However, oxidation with H_2O_2 at pH 7.3 but not 5.0 (Figure 3B) reduced the size of PS-A, albeit to a somewhat larger MW than APC-processed PS-A (Figure 2A, arrow). Furthermore, $NaIO_4$ (Figure 3C) as well as O_3 (Figure 3D) treatments were more effective at PS-A depolymerization, yielding polysaccharides that were the same MW as those found inside APCs (Figures 3C and 3D, arrows). Like H_2O_2, the $NaIO_4$ treatment worked best at pH 7.3, and O_3 treatment produced low MW PS-A in only 5 min (not shown), although reduction to ~15 kDa was optimal at 1 hr (Figure 3D).

To determine whether oxidation plays a significant role in ZPS processing in vivo and whether that processing is required for T cell activation, we compared the ability of WT C57BL/6, mice lacking the NADPH oxidase enzyme responsible for generating superoxide (CGD or chronic granulomatous disease model [Pollock et al., 1995]), and mice lacking inducible NO synthase (iNOS$^{-/-}$; Laubach et al., 1995) to develop abscesses against both *B. fragilis* and purified PS-A with SCC adjuvant. WT mice developed abscesses in response to either live *B. fragilis* bacteria or purified PS-A but not in response to adjuvant alone (Figure 4A). When challenged with *B. fragilis*, significantly fewer CGD and iNOS$^{-/-}$ mice developed abscesses than WT. However, when injected with purified PS-A, 100% of the CGD mice developed abscesses (Figure 4A) that were notably larger than those formed in WT animals (not shown), whereas most iNOS$^{-/-}$ mice failed to form abscesses (Figure 4A). Next, intact PS-A was compared to O_3-cleaved PS-A (~15 kDa) in abscess induction studies with WT and iNOS$^{-/-}$ mice. Although the intact PS-A did not induce abscesses in the iNOS$^{-/-}$ mice, the ability to elicit a T cell response leading to abscess formation was restored when O_3-cleaved PS-A was used (Figure 4B). No significant difference was seen between WT and iNOS$^{-/-}$ mice with O_3-cleaved PS-A (p = 0.6469).

Presentation of Polysaccharide Antigens Is Dependent upon MHC Class II Proteins

The cellular requirements to achieve ZPS uptake and presentation were further explored with confocal microscopy. Pixel histograms of Raji cells incubated with
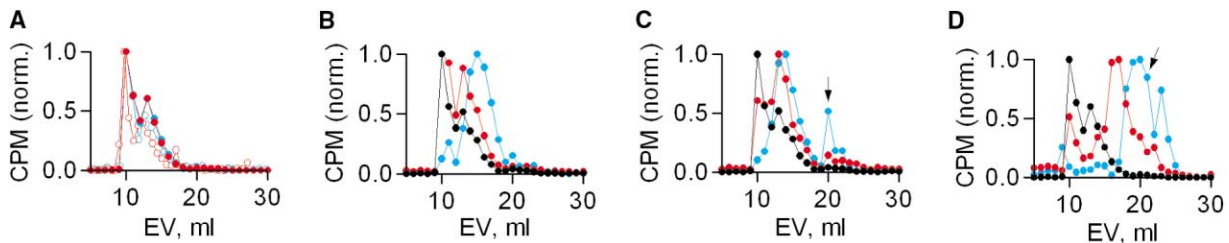

Figure 3. In Vitro ZPS Cleavage

Superose 12 elution profiles.

(A) pH (red) and 2-mercaptoethanol (blue) effects on PS-A MW. At both pH 5.0 (open circles) and 7.3 (solid circles), no change in MW was seen.

(B) 10% H_2O_2 at pH 5.0 (red) and pH 7.3 (blue) compared to control PS-A (black), showing only modest cleavage at pH 7.3 (MW $\gg$ 15 kDa).

(C) PS-A cleavage (MW $\geq$ 15 kDa; arrow) was seen with 1 mM $NaIO_4$ at pH 7.3 (blue), but not at pH 5.0 (red) or in the control (black).

(D) PS-A was treated by ozone gas for 0 (black), 30 (red), and 60 (blue) min, with most PS-A reduced to ~15 kDa (arrow) after 60 min.
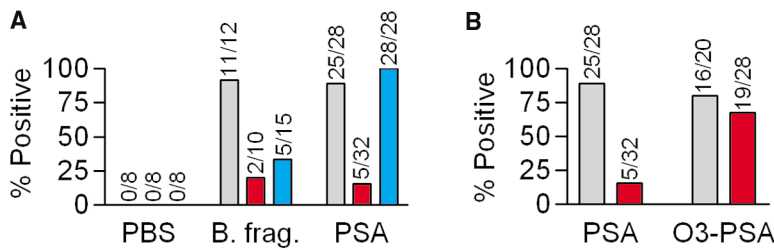
Figure 4. Abscess Formation

(A) Abscess induction in WT (gray), iNOS$^{-/-}$ (red), and CGD (blue) mice with either PBS, 10^8 live *B. fragilis*, or 50 μg PS-A with SCC adjuvant. Values listed are the number of abscess-positive animals per total. WT mice formed abscesses in response to both bacteria and purified PS-A whereas neither mutant developed abscesses against live bacteria. The CGD but not iNOS$^{-/-}$ mice formed abscesses against intact PS-A.

(B) WT (gray) and iNOS$^{-/-}$ (red) mice were challenged with intact or ozone-cleaved PS-A and SCC. Pre-cleavage of PS-A by ozone restored abscess formation in iNOS$^{-/-}$ mice. No significant difference with cleaved PS-A was seen in WT and iNOS$^{-/-}$ animals (p = 0.6469).

ZPS illustrate both the surface and intracellular PS-A (Figure 5A). These results were compared with those for Raji cells lacking MHCII expression (RJ2.2.5), Raji cells treated with colchicine, and Raji cells treated with BFA to determine the effects on surface localization. The RJ2.2.5 cells endocytosed PS-A, yet failed to present it on the cell surface (Figure 5B). Colchicine treatment of Raji cells blocked endocytosis of PS-A and prevented significant surface presentation (Figure 5C), while BFA blocked presentation but not uptake (Figure 5D). To confirm a direct interaction between ZPS and MHCII molecules, two approaches were taken. First, in vitro binding studies were performed with soluble HLA-DR2 protein and biotinylated ZPS molecules. At pH 5.0 (Figure 5E) and 7.3 (not shown), no detectable intact PS-A ($\geq$100 kDa) bound to HLA-DR2 either with or without HLA-DM. However, processed PS-A ($\sim$15 kDa) did bind to HLA-DR2 in the presence of HLA-DM, and this effect was reduced at pH 7.3 (Figure 5E). Second, co-IP experiments were performed using [^{3}H]-PSA with WT and iNOS$^{-/-}$ splenocytes and mAbs to MHCII to confirm that the in vitro binding data accurately reflect cellular presentation of PS-A and to correlate the abscess studies (Figure 4) with direct observations. Low MW PS-A antigen was observed in MHCII immunoprecipitates from WT cells, yet the iNOS$^{-/-}$ cells failed to present significant amounts of antigen (Figure 5F). Controls with LAMP-1 mAbs failed to co-IP PS-A, and SDS-treated PS-A controls showed no significant change in elution profile (not shown). The failure of iNOS$^{-/-}$ cells to present PS-A antigen was probed further using co-IP from WT and iNOS$^{-/-}$ cells incubated with both high and low MW PS-A (Figure 5G). Both cell populations presented low MW PS-A on MHCII molecules. The size of the PS-A precipitated was indistinguishable from that of the processed PS-A found inside APCs (Figure 2A).

Polysaccharide Antigens Induce APC/T Cell Engagement through MHCII and $\alpha\beta$TCR Proteins

The final step in the ZPS antigen pathway was analyzed by confocal microscopy in which mouse splenocytes from ZPS-treated mice were incubated without antigen, unlabeled PS-A, or a superantigen control and visualized using mAbs against MHCII and $\alpha\beta$TCRs to detect APC/T cell engagement. Without antigen (Figure 6A), no significant engagement was observed, yet the addition of unlabeled PS-A (Figure 6B) or superantigen (Figure 6C) induced engagement (<2% and >10%, respectively). The identity of the presented molecule was confirmed using fluorescent PS-A, yielding white colocalization of PS-A,

MHCII, and $\alpha\beta$TCR (Figures 6D–6F, arrows). No engagement was seen in cells from naïve mice (not shown).

Discussion

The Endocytic Pathway for Polysaccharide Antigens

The current paradigm for exogenous antigen presentation states that only proteins are taken into the endocytic pathway of APCs, localized to MIIC vesicles, processed by acid-activated proteases, exchanged onto MHCII proteins with the help of HLA-DM, and presented to T cells on the APC surface (Watts, 1997). Furthermore, polysaccharides are believed to be T cell-independent antigens. However, this mechanism does not account for the observations with ZPS antigens in that they elicit an MHCII-dependent CD4$^+$ T cell response that results in abscess formation (Tzianabos et al., 2000; Kalka-Moll et al., 2002). The current model for MHCII presentation does not explain these conflicting observations.

In the present report, we have shown that ZPS antigens behave remarkably similar to conventional protein antigens within the MHCII presentation pathway. First, endocytosis of PS-A was shown to be exquisitely controlled by cytoskeletal rearrangements. The specificity of this endocytosis and the possibility of receptor proteins remain unclear, although PS-A uptake by RJ2.2.5 cells and brefeldin A-treated Raji cells rules out MHCII and other ER-synthesized proteins as ZPS receptors. Nonetheless, nonspecific pinocytosis could be involved and thus the lack of T cell activation by neutral or singly charged polysaccharides (Tzianabos et al., 1993) likely reflects a lack of presentation or recognition rather than entry. Moreover, the delivery of lysosomal and exocytic vesicle contents to the endosome carrying ZPS antigens to form the MIIC vesicle has been demonstrated. Although these data effectively eliminate the possibility of an alternate ZPS presentation pathway in APCs, the entry mechanism differences between purified ZPS antigen and encapsulated bacteria during an infection remain to be elucidated.

We also document processing of ZPS antigens prior to presentation by MHCII. Previous reports demonstrated that very small ZPS antigens (<5 kDa; $\sim$5 repeating units) failed to activate T cells and induce abscess formation in mice, strongly suggesting a structural component to the immunogenicity of ZPS molecules beyond the zwitterionic charge motif of the repeating unit (Kalka-Moll et al., 2000). Interestingly, our binding, co-IP, and abscess induction results show that ZPS antigens must be processed to approximately 12–15 kDa ($\sim$15 re-
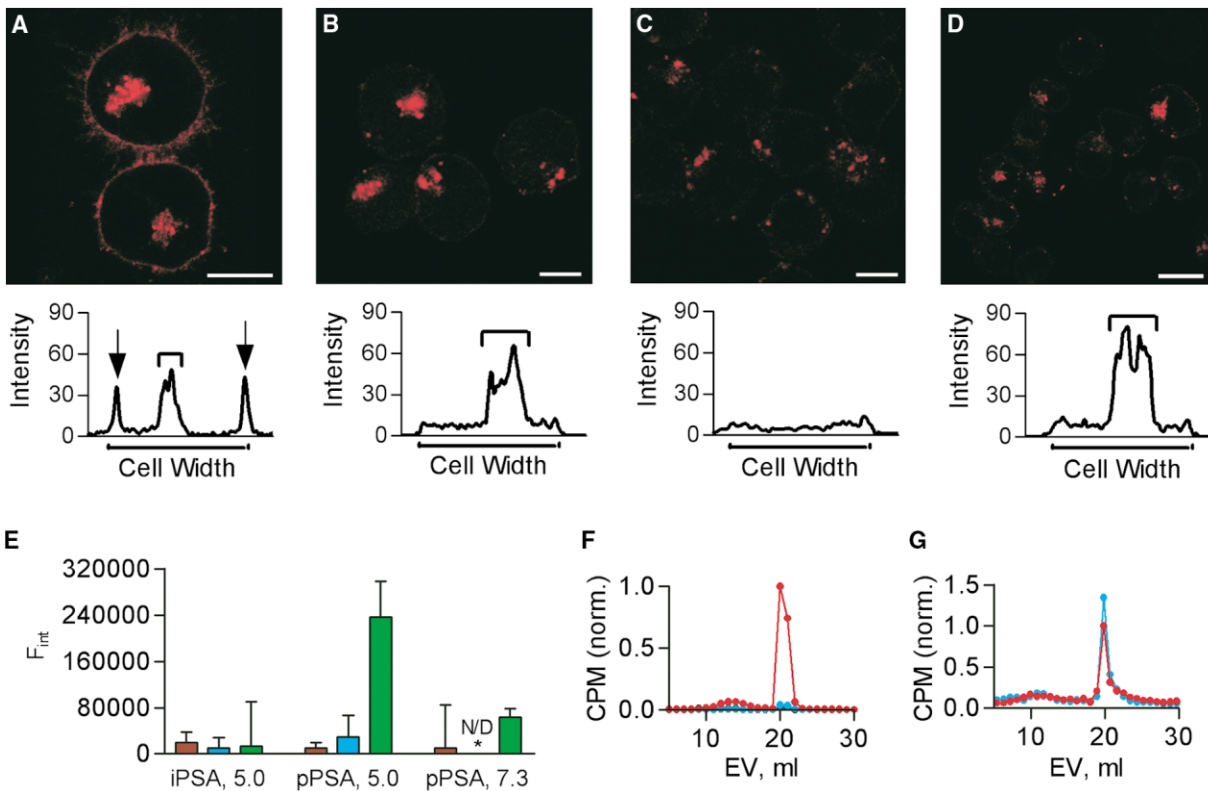
Figure 5. MHC-Dependent Presentation

White bars indicate 10 μm in each image and PS-A is red.

(A) PS-A with Raji cells, showing surface and internal PS-A. A pixel histogram shows the localization of PS-A.

(B) PS-A was incubated with RJ2.2.5 cells (MHCII$^{-/-}$ Raji cells) demonstrating that the lack of MHCII does not alter PS-A uptake but nearly eliminates surface-localized PS-A.

(C) PS-A with colchicine-treated Raji cells, showing that treatments results in an amount of surface PS-A comparable to that on RJ2.2.5 cells, but much less than untreated cells.

(D) PS-A with BFA-treated Raji cells. Uptake is unchanged, but surface localization is significantly reduced.

(E) Purified HLA-DR2 binding with either intact PS-A (iPSA) or 15 kDa PS-A (pPSA). The x axis indicates the ligand and pH. No binding is seen without HLA-DR2 (red), without HLA-DM added (blue), or with iPSA, yet pPSA was able to bind in a pH- and HLA-DM-sensitive manner (green).

(F) Intact PS-A co-IP with MHCII mAbs from WT and iNOS$^{-/-}$ splenocytes. Superose 12 analysis (EV = elution volume) revealed that low MW PS-A was bound to cellular MHCII molecules from WT (red) but not iNOS$^{-/-}$ (blue) cells. No PS-A was precipitated with LAMP-1 mAbs (black).

(G) A mixed MW population of PS-A co-IP with MHCII mAbs from WT and iNOS$^{-/-}$ splenocytes. Superose 12 analysis shows that both WT (red) and iNOS$^{-/-}$ (blue) cells exclusively bound and presented low MW PS-A. (F) and (G) show CPM values normalized to the highest WT count.

peating units) for presentation. Combined with the global helical conformation of ZPSs observed by NMR (Choi et al., 2002), these observations collectively suggest that these molecules must be long enough to maintain their helical conformation but small enough to allow stable binding to MHCII and recognition by αβTCRs without masking important protein-protein contacts.

Interestingly, no glycosidase activity capable of depolymerizing PS-A has been identified, yet we found that chemical oxidation by a number of oxidants effectively cleaved PS-A. Glycosidase enzymes are known to be very specific (Rye and Withers, 2000; Davies and Henrissat, 1995), yet all ZPS molecules, such as the type 8 capsule from *S. aureus* and Sp1, activate T cells in a manner indistinguishable from PS-A (Tzianabos et al., 1994, 2001). The use of a general processing mechanism via oxidation therefore fits well with the hypothesis that other ZPSs are also processed despite significant monosaccharide and linkage differences. In addition, the cleavage of PS-A by oxidation was possible only at a near-neutral pH but not at the acidic pH found later in the endocytic pathway; the implication is that if oxidation is the primary mechanism of ZPS processing, it must precede vesicular acidification.

With the involvement of oxidants, our model also fits well into the events surrounding the oxidative burst that accompanies phagocytosis of microbes. Upon uptake, APCs are known to produce large amounts of reactive oxygen species (ROS) and reactive nitrogen species (RNS) that facilitate bacterial killing (Forman and Torres, 2001). Experiments using the abscess induction model to measure in vivo T cell activation in superoxide-deficient (Pollock et al., 1995) and NO-deficient mice (Laubach et al., 1995) have yielded insights into the roles of these oxidation pathways. We found that ROS-deficient mice did not develop abscesses following live bacterial challenge, supporting the traditional notion that ROS oxidation plays a bactericidal function (Pollock et al., 1995). The killing of organisms results in liberation of their surface polysaccharides and internal proteins,
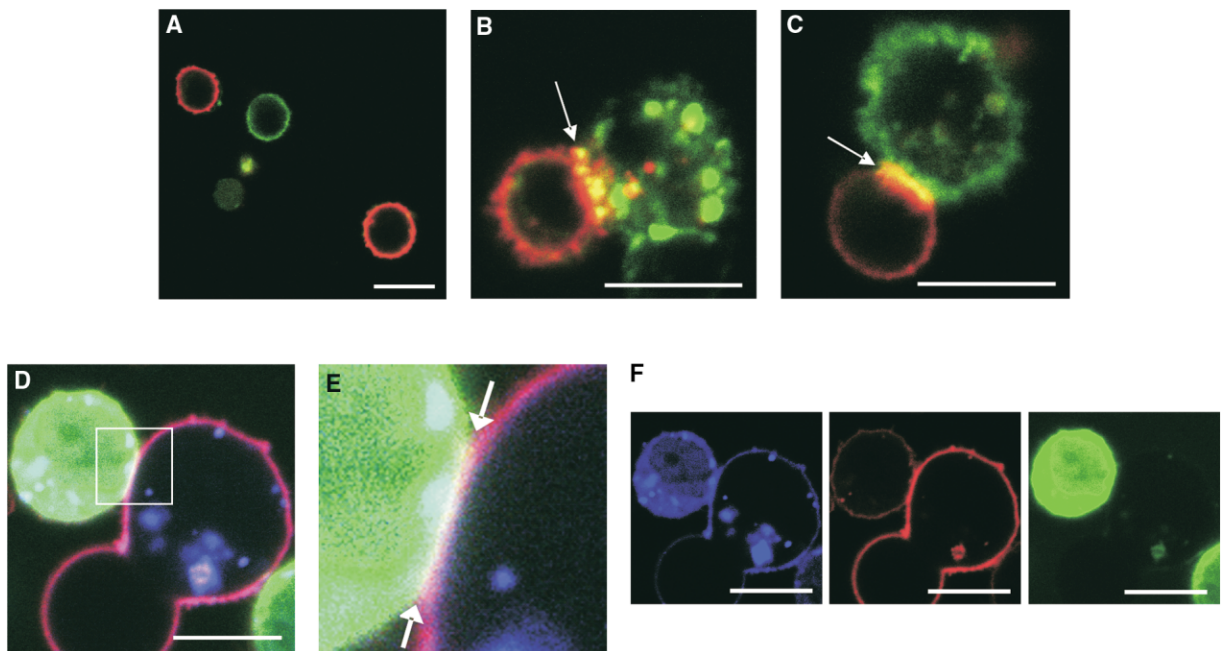
Figure 6. Immune Synapse Formation

Mouse splenocytes incubated with or without antigen and then stained for MHCII (red) and $\alpha\beta$TCR (green). White bars indicate 10 μm in each image. No APC/T cell engagement was seen in the absence of antigen (A); however, after incubation with unlabeled PS-A (B) or unlabeled superantigen (C), cells formed yellow immune synapses (arrows). (D) Tricolor analysis shows white trilocalization of PS-A (blue), MHCII (red), and $\alpha\beta$TCR (green) under the same conditions. (E) Magnification of (D) with colocalization (arrows). (F) Separate color channel images of (D) for clarity.

making these molecules available for processing and presentation. Consistent with this hypothesis was the robust abscess-inducing response mounted by ROS-deficient mice challenged with purified PS-A and SCC adjuvant. In contrast, mice lacking NO failed to form abscesses when challenged with either live bacteria or large MW PS-A (both containing SCC), implying that NO production is important not only for killing but also for molecular cleavage of capsular components. This possibility was explored in experiments which showed that iNOS$^{-/-}$ animals developed abscesses in response to low MW "pre-processed" PS-A with SCC. What's more, recent evidence shows that patients lacking superoxide produce significantly more NO than normal in response to inflammatory signals (Tsuji et al., 2002), providing an explanation as to why the CGD mice responded so strongly (100% formed abscesses) to intact ZPS challenge. These observations have led us to five conclusions. First, iNOS$^{-/-}$ mice have not lost the intrinsic ability to form abscesses in response to the appropriate stimuli. Second, iNOS$^{-/-}$ mice are incapable of processing PS-A for MHCII presentation. Third, the ROS and RNS pathways are not redundant in their contribution to ZPS uptake, processing, and presentation. Fourth, the activation of T cells occurs by ZPS presentation and is not a result of contaminating peptides, which can be presented by iNOS$^{-/-}$ mice. Finally, these results demonstrate conclusively that ZPS processing is necessary for T cell activation in vivo.

After oxidative processing and the formation of the MIIC, the vesicles undergo acidification (Watts, 1997). Previous reports have demonstrated that blockade of

acidification inhibits ZPS-mediated T cell activation (Kalka-Moll et al., 2002), therefore if processing of ZPS molecules requires near-neutral pH and is not dependent upon enzymatic activity, then acidification must remain critical for other reasons. It is conceivable that protease activity is still important because of the action of cathepsin S and its role in Ii cleavage (Riese et al., 1998). This cleavage event is essential to allow antigenic peptides to bind MHCII for presentation. In addition, the function of the exchange factor HLA-DM is pH sensitive in that it requires a low pH for activity (Busch et al., 1998). Without Ii cleavage and peptide exchange, the binding groove on MHCII is not available to conventional antigens. In ongoing studies, we have found that knockout mice lacking H2-M (murine HLA-DM homolog) do not develop abscesses when challenged with ZPS (D.L.K., unpublished data). The present data suggest that ZPS molecules require Ii cleavage and CLIP exchange by HLA-DM in order to free the necessary binding site for ZPS antigens. The implication is that ZPS and CLIP peptide binding to MHCII appear to be mutually exclusive.

One major difference between superantigens and conventional antigens is the requirement for endocytic pathway. Superantigens merely bind to MHCII proteins on the surface of the APC, where they are recognized by $\alpha\beta$TCR proteins on T cells (Kappler et al., 1994). Conventional antigens, however, require passage through the endocytic pathway in order to be processed and loaded onto MHCII inside the cell prior to surface exposure and T cell recognition (Watts, 1997; Watts and Powis, 1999). Our confocal data demonstrate that with-
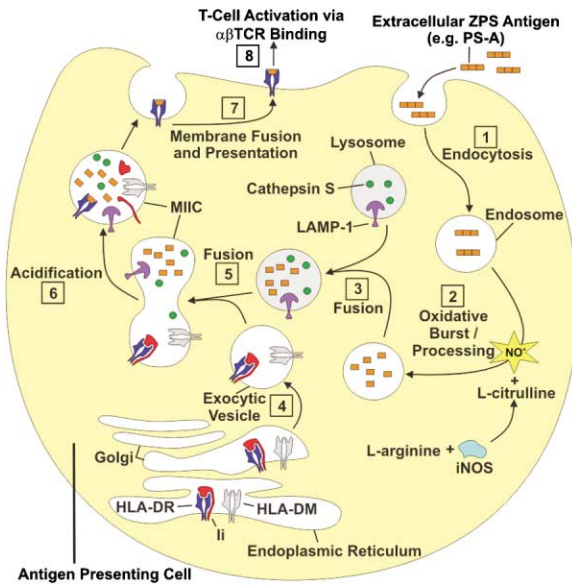
Figure 7. MHCII Pathway Model for ZPS Antigens

Schematic model illustrating the key steps in the ZPS/MHCII pathway. [1] Extracellular antigens are endocytosed for presentation through a cytoskeleton-dependent mechanism. [2] Cells undergo an oxidative burst, including the production of NO. NO and potentially other oxidants process the antigen to low MW polysaccharides. [3] Endosomes fuse with resident lysosomes. [4] The MHC proteins HLA-DR, HLA-DM, and Ii are assembled in the ER, transported through the Golgi apparatus, and then budded into exocytic vesicles. [5] Antigen-rich endo/lysosomes fuse with exocytic vesicles, creating the MIIC vesicle carrying HLA-DR, HLA-DM, LAMP-1, and antigen. MIIC acidification activates proteases responsible for processing protein antigens and cleavage of Ii, thus permitting the HLA-DM-mediated antigen exchange of CLIP. [7] Processed antigens are loaded onto MHC with the help of HLA-DM and then shuttled to the cell surface for recognition by αβTCRs. [8] ZPS molecules mediate APC/T cell engagement through αβTCR recognition.

out entry into B cells, PS-A does not accumulate on the cell surface, which agrees with the previous reports showing that fixed APCs fail to activate T cells with ZPS antigens (Brubaker et al., 1999). In addition, HLA-DM inhibition or a lack of MHCII expression results in uptake without presentation. These data solidify the importance of MHCII expression, the removal of peptides from the MHCII binding groove, and the general requirement for PS-A to enter the APC. However, confocal microscopy and immunogold-EM (Kalka-Moll et al., 2002) colocalization studies lack the necessary resolution to measure direct macromolecular interactions.

In vitro binding assays demonstrated that only low MW PS-A interacted with HLA-DR2, a result suggesting that processing is required for presentation. Furthermore, we found that this interaction was dependent upon HLA-DM and low pH, supporting the lack of presentation by B cells in the presence of BFA and chloroquine as well as previous studies showing no T cell activation mediated by BFA-treated APCs (Kalka-Moll et al., 2002). Moreover, co-IP results conclusively show that only low MW ZPS antigen were presented by MHCII proteins and that the production of NO is critical for the processing of ZPS molecules prior to MHCII loading. These data, obtained from live APCs, provide a critical

link for the cellular and in vitro processing data, the animal abscess results, and the quantitative in vitro binding data. In fact, these results provide a logical biochemical explanation for the abscess induction results by showing that only low MW ZPS can be presented by MHCII proteins, that NO is required to accomplish this processing, and that this defect can be overcome by pre-processing of the input ZPS antigen. Lastly, we show T cell and APC engagement in direct response to PS-A presentation by APCs via interactions with MHCII and αβTCRs, confirming that the alternate CD1/γδTCR pathway is not involved with ZPS immune responses. These data collectively demonstrate a direct and functional interaction between MHCII, NO-processed ZPS molecules, and αβTCRs that leads to T cell activation and abscess formation.

The Model and Its Implications

This report documents ZPS oxidative processing and the use of the MHCII endocytic pathway by a non-protein antigen prior to its presentation and recognition. We therefore propose a model to illustrate our findings in the context of the known MHCII endocytic pathway (Figure 7).

One particular area of impact of our findings is the role of NO in host immune responses. Production of NO has been shown to be important in many situations in vivo, ranging from neurotransmission (Koh et al., 2001) to vasodilation (Edmunds and Marshall, 2003). Many studies have demonstrated that loss of NO production during inflammation can lead to immune suppression and an increase in bacterial infections (Gantt et al., 2001). Our results show that absence of NO production during inflammation would be inhibitory to T cell activation by carbohydrate antigens, which may in part explain some of the alterations in immunity seen during inflammation.

Due to the fact that many extracellular pathogens have carbohydrate surfaces, the ability of ZPS molecules to activate T cells through MHCII presentation offers significant opportunities for the design of new classes of vaccines against a variety of infectious diseases. Interestingly, the ability of ZPSs to utilize this pathway for presentation to T cells may begin to explain why immunization of humans with some polysaccharide vaccines elicits a significant IgG response (Pier and Elcock, 1984)—a result that does not fit the paradigm of T cell-independent IgM production. Indeed, the present study underscores the capacity of the cellular immune system to recognize a broader spectrum of pathogenic organisms and molecules than previously believed.

Experimental Procedures

Cell Lines and Culturing
C57BL/6 mouse splenocytes from PS-A-primed mice (50 μg IP on days −8 and −1) and human PBMCs were isolated with a Ficoll-Hypaque gradient as before (Tzianabos et al., 2000). Cell preparations were enriched for T cells by nylon wool. For confocal studies, human lymphoma B cell line Raji and MHCII$^{-/-}$ Raji cells (RJ2.5; (Accolla et al., 1985) were used. Processing studies used Raji cells, murine M12 B cells (gift from E. Kieff, Brigham & Women's Hospital), human THP-1 monocytes (ATCC), and mouse B1 B cells (WEHI-231; ATCC). Cells were cultured in either RPMI1640 or Dulbecco's

Modified Eagle Medium (ATCC) supplemented with 10% fetal bovine serum.(GIBCO, Grand Island, New York).

ZPS Purification
PS-A was purified from a mutant *B. fragilis* strain producing only PS-A in its capsule (Krinos et al., 2001). Bacteria growth and PS-A purification were performed as previously described (Tzianabos et al., 1992). The final PS-A sample was characterized by SDS-PAGE, H^1-NMR spectroscopy, Western blots, and wavelength scans. The final preparation was judged to be >99% pure by these methods.

ZPS Labeling
PS-A was oxidized with $NaIO_4$ so that 20% of the galactofuranose side chain sugar was modified to contain an aldehyde at the C5 position. Hydrazide-linked AlexaFluor®594 (Molecular Probes, Eugene, Oregon) and biotin (Pierce, Rockford, Illinois) tags were attached to the aldehyde according to the manufacturer's specifications. For radiolabeling, the aldehyde was reduced by [^{3}H]-$NaBH_4$.

ZPS Antigen Uptake, Colocalization, and Image Analysis
Texas Red conjugated dextran (70 kDa) and ovalbumin were from Molecular Probes. Monoclonal mAbs (PharMingen, San Diego, California, except as indicated) to human LAMP-1 (clone H4A3), human HLA-DR2 (clone L243; purified from HB-55 hybridoma; ATCC), human HLA-DM (clone MaP.DM.1), murine I-A^d/I-E^d (clone 2G9), and human (clone T10B9.1A-31) and murine (clone H57-597) αβTCR were conjugated to AlexaFluor®488 (Molecular Probes). Raji cells (10^6) were incubated with 50 μg of conjugated PS-A for 3 hr at 37°C in a water-jacketed incubator with 5% CO_2 and then fixed in 4% paraformaldehyde for 30 min at RT. Cells were incubated with antibody for 30 min and then visualized with a Zeiss Pascal confocal microscope (63× objective lens; Carl Zeiss, Thornwood, New York). Cross-sectional histograms of the pixel intensities were created from high-resolution confocal images by image analysis software (Diversity Database v. 2.2.0, BioRad, Hercules, California). Other antigen controls (not shown) included ovalbumin, 70 kDa dextran, 10 kDa dextran, 40 kDa dextran sulfate, and type 3 group B streptococcal capsular polysaccharide. Amounts incubated with Raji cells were equimolar to 50 μg of PS-A.

Drug Treatments
Raji cells were treated for 1 hr with colchicine (10 μM), cytochalasin D (20 μM), BFA (100 nM), or chloroquine (200 μg/ml) prior to incubation with PS-A. Brefeldin A (2.5, 5.0, and 20 μg/ml) was added 30 min before PS-A. For semiquantitative analysis, cells were manually counted for total cells and cells positive for colocalization in all images taken (n > 5) for each drug treatment and concentration used. Drug-free controls were performed for comparison. Statistical evaluation was performed with an unpaired Student's t test at a 95% confidence level (Prism v. 3.0, GraphPad, San Diego, California).

In Vitro Processing Assays
APCs (10^8) were cultured in the presence of 0.5 mg of [^{3}H]-PSA for 15 to 18 hr. at 37°C to allow uptake and processing. Cells were collected and washed with PBS. Cell lysis was performed by passage through a 27 gauge needle in 250 mM sucrose with 50 mM Tris-HCl, pH 7.5. Microsomes were isolated for analysis of ingested PS-A with centrifugation (Schroter et al., 1999). The pellet was then digested with Pronase to eliminate contaminating protein. The presence of microsomal markers (HLA-DM and LAMP-1) were verified in non-Pronase digested pellets by ELISA (not shown). Microsomal PS-A was analyzed by molecular sieve chromatography on a Superose 12 column in PBS using a BioRad FPLC (BioLogic HR, BioRad). Fractions were assayed for radioactivity to determine the elution profile.

Microsomal lysates not digested with Pronase were also assayed for protease and glycosidase activity. Glycosidase activity was assessed by incubation microsomal lysates with [^{3}H]-PSA at pH 5.0 and 7.3 in a dual-buffered system (A/PBS; 50 mM sodium acetate, 50 mM sodium monobasic phosphate, 0.9% NaCl). Degradation was determined by Superose 12 chromatography. For controls, protease activity was measured in a casein assay (Molecular Probes) at pH 5.0 and 7.3 in A/PBS buffer and was compared to trypsin (Sigma, St. Louis, Missouri).

In vitro degradation was performed by incubation of [^{3}H]-PSA under various solution conditions overnight at 37°C. Degradation was assessed by Superose 12 chromatography.

Binding Assays
CHO cells producing soluble HLA-DR2 (Gauthier et al., 1998) with a peptide from myelin basic protein (residues 85–99) on the amino terminus of the β subunit were used as a source of MHCII protein. MAbs to HLA-DR were purified from HB-55 hybridoma medium and conjugated to affinity resin. Cells were grown at high density in serum-free medium (HyQ® SFM4CHO, HyClone, Logan, Utah), and secreted protein was purified from the spent medium using affinity chromatography and was judged to be >99% homogeneous by SDS-PAGE and Coomassie blue staining. Protein was digested with thrombin (Sigma) for 1 hr to cleave the peptide bond holding the peptide to the β chain, enabling antigen exchange and binding.

Biotinylated intact PS-A (>100 kDa) or ozone-cleaved PS-A (~15 kDa) was incubated at 5 μM in ELISA plate wells (Immulon 2 HB, Fisher Scientific, Pittsburgh, Pennsylvania) coated with either glycine (negative control) or purified HLA-DR2 (100 ng/well) for 24 hr at 37°C with mild agitation in A/PBS. In some assays, purified soluble HLA-DM (gift from S. DeWall, Harvard Medical School) (Mosyak et al., 1998) was also added (1 μg/well). Bound PS-A was detected with europium-conjugated streptavidin, DELFIA® Enhancement Buffer (according to the manufacturer's specifications; Perkin-Elmer, Boston, Massachusetts), and time-resolved fluorescence measurements in a Wallac Victor² plate fluorometer (Perkin-Elmer). Background from the glycine negative controls at each condition was subtracted from the raw data.

Abscess Induction Studies
All mice were obtained from Jackson Laboratories (Bar Harbor, Maine). Strains were as follows: WT mice, strain C57BL/6J, stock 000664; CGD mice on C57BL/6 background, strain B6.129S6-*Cybb*^{tm1Din}, stock 002365 (Pollock et al., 1995); and iNOS$^{-/-}$ mice on C57BL/6 background, strain B6.129P2-*Nos2*^{tm1Lau}, stock 002609 (Laubach et al., 1995). Abscess induction was perform as before (Tzianabos et al., 1999), with live *B. fragilis* (10^8 cfu/injection) or purified PS-A (50 μg/mouse). Animals were examined for the presence of one or more abscesses 6 days after challenge.

Coimmunoprecipitations
Spleens (n = 12) were harvested from either WT C57BL/6 or iNOS$^{-/-}$ mice. Mononuclear cells were incubated for 24 hr at 37°C with 1 mg of either intact (>100,000 kDa) or a mixture of high and low MW [^{3}H]-PSA (>100,000 kDa to <10 kDa). Cells were then digested with papain (0.1 mg/ml papain; 10 mM Tris-HCl, pH 7.5; 1 mM EDTA; 1% β-mercaptoethanol) for 1 hr at 37°C to release the MHCII proteins from the plasma membrane (Wiman et al., 1982). The supernatants were added to protein A-agarose beads (Sigma) containing 25 μg of mAb to either MHCII (clone 2G9, PharMingen, San Diego, California) or LAMP-1 (clone 1D4B, PharMingen) and protease inhibitor cocktail (Sigma) and incubated overnight with mixing at 4°C. The resin was boiled in 10% SDS with 10% β-mercaptoethanol and 3 M NaCl for 20 min. The supernatants were analyzed by Superose 12 chromatography and fractions analyzed for radioactivity.

APC/T Cell Engagement
For dual-stained T cell engagement studies, T cell-enriched splenocytes from PS-A-injected (50 μg/animal, IP, days −7 and −1) WT C57BL/6 mice (Jackson Labs) were incubated with unlabeled antigen (staphylococcal enterotoxin A at 10 ng/ml, PS-A at 50 μg/ml, or medium-only control) for 3 days at 37°C. The cell populations were then transferred to poly-L lysine-coated slides and stained for 30 min at 4°C with AlexaFluor®594-conjugated mAbs to murine MHCII and AlexaFluor®488 antibody to the αβTCR. Confocal images were collected as described above. Tricolor T cell engagement studies were done exactly as specified above, only using Alexa-Fluor®594-conjugated PS-A at 50 μg/ml with AlexaFluor®488 antibody to murine MHCII and AlexaFluor®633-conjugated antibody to the αβTCR. In order to reduce confusion, the signal from PS-A was

assigned to the blue channel, murine MHCII to red, and $\alpha\beta$TCR to green.

References

Abbas, A.K., Lichtman, A.H., and Pober, J.S. (2000). Cellular and Molecular Immunology (New York: W.B. Saunders Company).

Accolla, R.S., Carra, G., Buchegger, F., Carrel, S., and Mach, J.P. (1985). The human Ia-associated invariant chain is synthesized in Ia-negative B cell variants and is not expressed on the cell surface of both Ia-negative and Ia-positive parental cells. J. Immunol. *134*, 3265–3271.

Adorini, L., Ullrich, S.J., Appella, E., and Fuchs, S. (1990). Inhibition by brefeldin A of presentation of exogenous protein antigens to MHC class II-restricted T cells. Nature *346*, 63–66.

Bacci, S., Nakamura, T., and Streilein, J.W. (1996). Failed antigen presentation after UVB radiation correlates with modifications of Langerhans cell cytoskeleton. J. Invest. Dermatol. *107*, 838–843.

Baker, C.J., Paoletti, L.C., Wessels, M.R., Guttormsen, H.K., Rench, M.A., Hickman, M.E., and Kasper, D.L. (1999). Safety and immunogenicity of capsular polysaccharide-tetanus toxoid conjugate vaccines for group B streptococcal types Ia and Ib. J. Infect. Dis. *179*, 142–150.

Brubaker, J.O., Li, Q., Tzianabos, A.O., Kasper, D.L., and Finberg, R.W. (1999). Mitogenic activity of purified capsular polysaccharide A from Bacteroides fragilis: differential stimulatory effect on mouse and rat lymphocytes in vitro. J. Immunol. *162*, 2235–2242.

Busch, R., Reich, Z., Zaller, D.M., Sloan, V., and Mellins, E.D. (1998). Secondary structure composition and pH-dependent conformational changes of soluble recombinant HLA-DM. J. Biol. Chem. *273*, 27557–27564.

Choi, Y.H., Roehrl, M.H., Kasper, D.L., and Wang, J.Y. (2002). A unique structural pattern shared by T-cell-activating and abscess-regulating zwitterionic polysaccharides. Biochemistry *41*, 15144–15151.

Chung, D.R., Kasper, D.L., Panzo, R.J., Chtinis, T., Grusby, M.J., Sayegh, M.H., and Tzianabos, A.O. (2003). CD4+ T cells mediate abscess formation in intra-abdominal sepsis by an IL-17-dependent mechanism. J. Immunol. *170*, 1958–1963.

D'Souza, M.P., and August, J.T. (1986). A kinetic analysis of biosynthesis and localization of a lysosome-associated membrane glycoprotein. Arch. Biochem. Biophys. *249*, 522–532.

Davies, G., and Henrissat, B. (1995). Structures and mechanisms of glycosyl hydrolases. Structure *3*, 853–859.

Edmunds, N.J., and Marshall, J.M. (2003). The roles of nitric oxide in dilating proximal and terminal arterioles of skeletal muscle during systemic hypoxia. J. Vasc. Res. *40*, 68–76.

Forman, H.J., and Torres, M. (2001). Redox signaling in macrophages. Mol. Aspects Med. *22*, 189–216.

Gantt, K.R., Goldman, T.L., McCormick, M.L., Miller, M.A., Jeronimo, S.M., Nascimento, E.T., Britigan, B.E., and Wilson, M.E. (2001). Oxidative responses of human and murine macrophages during phagocytosis of Leishmania chagasi. J. Immunol. *167*, 893–901.

Gauthier, L., Smith, K.J., Pyrdol, J., Kalandadze, A., Strominger, J.L., Wiley, D.C., and Wucherpfennig, K.W. (1998). Expression and crystallization of the complex of HLA-DR2 (DRA, DRB1*1501) and an immunodominant peptide of human myelin basic protein. Proc. Natl. Acad. Sci. USA *95*, 11828–11833.

Kalka-Moll, W.M., Tzianabos, A.O., Wang, Y., Carey, V.J., Finberg, R.W., Onderdonk, A.B., and Kasper, D.L. (2000). Effect of molecular size on the ability of zwitterionic polysaccharides to stimulate cellular immunity. J. Immunol. *164*, 719–724.

Kalka-Moll, W.M., Tzianabos, A.O., Bryant, P.W., Niemeyer, M., Ploegh, H.L., and Kasper, D.L. (2002). Zwitterionic polysaccharides stimulate T cells by MHC class II-dependent interactions. J. Immunol. *169*, 6149–6153.

Kappler, J., White, J., Kozono, H., Clements, J., and Marrack, P. (1994). Binding of a soluble alpha beta T-cell receptor to superantigen/major histocompatibility complex ligands. Proc. Natl. Acad. Sci. USA *91*, 8462–8466.

Kasper, D.L., Paoletti, L.C., Wessels, M.R., Guttormsen, H.K., Carey, V.J., Jennings, H.J., and Baker, C.J. (1996). Immune response to type III group B streptococcal polysaccharide-tetanus toxoid conjugate vaccine. J. Clin. Invest. *98*, 2308–2314.

Koh, S.D., Monaghan, K., Sergeant, G.P., Ro, S., Walker, R.L., Sanders, K.M., and Horowitz, B. (2001). TREK-1 regulation by nitric oxide and cGMP-dependent protein kinase. An essential role in smooth muscle inhibitory neurotransmission. J. Biol. Chem. *276*, 44338–44346.

Krinos, C.M., Coyne, M.J., Weinacht, K.G., Tzianabos, A.O., Kasper, D.L., and Comstock, L.E. (2001). Extensive surface diversity of a commensal microorganism by multiple DNA inversions. Nature *414*, 555–558.

Laubach, V.E., Shesely, E.G., Smithies, O., and Sherman, P.A. (1995). Mice lacking inducible nitric oxide synthase are not resistant to lipopolysaccharide-induced death. Proc. Natl. Acad. Sci. USA *92*, 10688–10692.

Mosyak, L., Zaller, D.M., and Wiley, D.C. (1998). The structure of HLA-DM, the peptide exchange catalyst that loads antigen onto class II MHC molecules during antigen presentation. Immunity *9*, 377–383.

Pier, G.B., and Elcock, M.E. (1984). Nonspecific immunoglobulin synthesis and elevated IgG levels in rabbits immunized with mucoid exopolysaccharide from cystic fibrosis isolates of Pseudomonas aeruginosa. J. Immunol. *133*, 734–739.

Pollock, J.D., Williams, D.A., Gifford, M.A., Li, L.L., Du, X., Fisherman, J., Orkin, S.H., Doerschuk, C.M., and Dinauer, M.C. (1995). Mouse model of X-linked chronic granulomatous disease, an inherited defect in phagocyte superoxide production. Nat. Genet. *9*, 202–209.

Riberdy, J.M., Newcomb, J.R., Surman, M.J., Barbosa, J.A., and Cresswell, P. (1992). HLA-DR molecules from an antigen-processing mutant cell line are associated with invariant chain peptides. Nature *360*, 474–477.

Riese, R.J., Mitchell, R.N., Villadangos, J.A., Shi, G.P., Palmer, J.T., Karp, E.R., De Sanctis, G.T., Ploegh, H.L., and Chapman, H.A. (1998). Cathepsin S activity regulates antigen presentation and immunity. J. Clin. Invest. *101*, 2351–2363.

Rotzschke, O., Lau, J.M., Hofstatter, M., Falk, K., and Strominger, J.L. (2002). A pH-sensitive histidine residue as control element for ligand release from HLA-DR molecules. Proc. Natl. Acad. Sci. USA *99*, 16946–16950.

Rye, C.S., and Withers, S.G. (2000). Glycosidase mechanisms. Curr. Opin. Chem. Biol. *4*, 573–580.

Sanderson, F., Kleijmeer, M.J., Kelly, A., Verwoerd, D., Tulp, A., Neefjes, J.J., Geuze, H.J., and Trowsdale, J. (1994). Accumulation of HLA-DM, a regulator of antigen presentation, in MHC class II compartments. Science *266*, 1566–1569.

Schroter, C.J., Braun, M., Englert, J., Beck, H., Schmid, H., and Kalbacher, H. (1999). A rapid method to separate endosomes from lysosomal contents using differential centrifugation and hypotonic lysis of lysosomes. J. Immunol. Methods *227*, 161–168.

Shi, G.P., Munger, J.S., Meara, J.P., Rich, D.H., and Chapman, H.A. (1992). Molecular cloning and expression of human alveolar macrophage cathepsin S, an elastinolytic cysteine protease. J. Biol. Chem. *267*, 7258–7262.

Shi, G.P., Villadangos, J.A., Dranoff, G., Small, C., Gu, L., Haley, K.J., Riese, R., Ploegh, H.L., and Chapman, H.A. (1999). Cathepsin S required for normal MHC class II peptide loading and germinal center development. Immunity 10, 197–206.

Sloan, V.S., Cameron, P., Porter, G., Gammon, M., Amaya, M., Mellins, E., and Zaller, D.M. (1995). Mediation by HLA-DM of dissociation of peptides from HLA-DR. Nature 375, 802–806.

Svensson, M., Stockinger, B., and Wick, M.J. (1997). Bone marrow-derived dendritic cells can process bacteria for MHC-I and MHC-II presentation to T cells. J. Immunol. 158, 4229–4236.

Tsuji, S., Taniuchi, S., Hasui, M., Yamamoto, A., and Kobayashi, Y. (2002). Increased nitric oxide production by neutrophils from patients with chronic granulomatous disease on trimethoprim-sulfamethoxazole. Nitric Oxide 7, 283–288.

Tzianabos, A.O., and Kasper, D.L. (2002). Role of T cells in abscess formation. Curr. Opin. Microbiol. 5, 92–96.

Tzianabos, A.O., Pantosti, A., Baumann, H., Brisson, J.R., Jennings, H.J., and Kasper, D.L. (1992). The capsular polysaccharide of Bacteroides fragilis comprises two ionically linked polysaccharides. J. Biol. Chem. 267, 18230–18235.

Tzianabos, A.O., Onderdonk, A.B., Rosner, B., Cisneros, R.L., and Kasper, D.L. (1993). Structural features of polysaccharides that induce intra-abdominal abscesses. Science 262, 416–419.

Tzianabos, A.O., Onderdonk, A.B., Zaleznik, D.F., Smith, R.S., and Kasper, D.L. (1994). Structural characteristics of polysaccharides that induce protection against intra-abdominal abscess formation. Infect. Immun. 62, 4881–4886.

Tzianabos, A.O., Russell, P.R., Onderdonk, A.B., Gibson, F.C., III, Cywes, C., Chan, M., Finberg, R.W., and Kasper, D.L. (1999). IL-2 mediates protection against abscess formation in an experimental model of sepsis. J. Immunol. 163, 893–897.

Tzianabos, A.O., Finberg, R.W., Wang, Y., Chan, M., Onderdonk, A.B., Jennings, H.J., and Kasper, D.L. (2000). T cells activated by zwitterionic molecules prevent abscesses induced by pathogenic bacteria. J. Biol. Chem. 275, 6733–6740.

Tzianabos, A.O., Wang, J.Y., and Lee, J.C. (2001). Structural rationale for the modulation of abscess formation by Staphylococcus aureus capsular polysaccharides. Proc. Natl. Acad. Sci. USA 98, 9365–9370.

Wang, Y., Kalka-Moll, W.M., Roehrl, M.H., and Kasper, D.L. (2000). Structural basis of the abscess-modulating polysaccharide A2 from Bacteroides fragilis. Proc. Natl. Acad. Sci. USA 97, 13478–13483.

Watts, C. (1997). Capture and processing of exogenous antigens for presentation on MHC molecules. Annu. Rev. Immunol. 15, 821–850.

Watts, C., and Powis, S. (1999). Pathways of antigen processing and presentation. Rev. Immunogenet. 1, 60–74.

Wiman, K., Claesson, L., Rask, L., Tragardh, L., and Peterson, P.A. (1982). Purification and partial amino acid sequence of papain-solubilized class II transplantation antigens. Biochemistry 21, 5351–5358.